Oxygen K-edge electron energy loss spectra of hydrous and anhydrous compounds

2013 J. Phys.: Condens. Matter 25 485401

(http://iopscience.iop.org/0953-8984/25/48/485401)

OPEN ACCESS

Made open access 14 January 2014

IOP PUBLISHING

JOURNAL OF PHYSICS: CONDENSED MATTER

J. Phys.: Condens. Matter **25** (2013) 485401 (5pp)

doi:10.1088/0953-8984/25/48/485401

Oxygen K-edge electron energy loss spectra of hydrous and anhydrous compounds

B Winkler[1], M Avalos-Borja[2,6], V Milman[3], A Perlov[3], C J Pickard[4] and J R Yates[5]

[1] Geowissenschaften, Goethe-Universität, Altenhoeferallee 1, D-60438 Frankfurt a.M., Germany
[2] Centro de Nanociencias y Nanotecnología, Universidad Nacional Autónoma de México (UNAM), Ensenada, Mexico
[3] Accelrys, 334 Science Park, Cambridge CB4 0WN, UK
[4] Department of Physics and Astronomy, University College London, Gower Street, London WC1E 6BT, UK
[5] Department of Materials, University of Oxford, Parks Road, Oxford OX1 3PH, UK

E-mail: b.winkler@kristall.uni-frankfurt.de

Received 22 July 2013, in final form 6 October 2013
Published 30 October 2013
Online at stacks.iop.org/JPhysCM/25/485401

Abstract

First-principles calculations have been employed to examine the possible use of electron energy loss spectroscopy (EELS) as a tool for determining the presence of OH groups and hence hydrogen content in compounds. Our density functional theory (DFT) based calculations describe accurately the experimental EELS results for forsterite (Mg_2SiO_4), hambergite ($Be_2BO_3(OH)$), brucite ($Mg(OH)_2$) and diaspore (α-AlOOH). DFT calculations were complemented by an experimental time resolved study of the oxygen K-edge in diaspore. The results show unambiguously that there is no connection between a pre-edge feature in the oxygen K-edge spectrum of diaspore and the presence of OH groups in the structure. Instead, the experimental study shows that the pre-edge feature in diaspore is transient. It can be explained by the presence of molecular O_2, which is produced as a result of the electron irradiation.

(Some figures may appear in colour only in the online journal)

1. Introduction

It was first claimed by Wirth (1997) that the presence of hydrogen bound to oxygen could be detected in compounds by electron energy loss spectroscopy (EELS) through the observation of a pre-edge feature at energies of ≈528 eV. This interpretation of the electron energy loss (EEL) spectra was immediately challenged (van Aken *et al* 1998, Wirth 1998). While numerous applications of this approach have been presented (see references in Garvie (2010)), alternative explanations of the origin of the 'pre-peak' feature have been brought forward (e.g. van Aken *et al* 1998, Jiang 2006, Garvie 2010). Specifically, time resolved EELS studies seem to indicate that under electron irradiation in the TEM, a transient peak near 530 eV may be observed in H-bearing as well as anhydrous minerals. This peak has been associated with an electron transition in molecular O_2, which is thought to be liberated due to damage induced by the incident electron beam (Jiang 2006, Garvie 2010).

Early theoretical approaches (van Aken *et al* 1999) did not support the claim by Wirth (1997), but the agreement of the spectra from the model calculations with experiment was only moderate. More recently, however, based on the work by Pickard and Payne (1997), the computation of EEL spectra in the framework of density functional theory models has become feasible, where the flexibility of mature

[6] On leave at: IPICyT, División de Materiales Avanzados, San Luis Potosí, S.L.P., Mexico.

plane wave/pseudopotential based approaches, which allow complex geometries to be optimized, is combined with the capability to include the effect of core holes. In fact, an example of a computed EEL spectrum addressing the question of whether a pre-peak feature is characteristic for hydroxy-apatite has been presented by Gao *et al* (2009). However, in that study the experimental spectrum was not well reproduced and it was necessary to perform the calculations using a supercell approximating the disordered structure.

The present study proceeds by demonstrating the accuracy of DFT based calculations of electron energy loss spectra for the oxygen K-edge. The first compound chosen for this benchmark is hambergite, $Be_2BO_3(OH)$, because it has four symmetrically independent oxygen atoms, three of which participate in the coordination of boron in planar BO_3 groups, while one is part of an OH group. There is no disorder or partial occupation of Wyckoff positions and the EELS shows a very distinct oxygen K-edge spectrum with two well separated main maxima (Garvie 2010). We also compute the EEL spectrum of forsterite, Mg_2SiO_4, which has three symmetrically independent oxygen positions, but no OH groups, and where the EEL spectrum shows a distinct double maximum (Garvie 2010). In contrast, in brucite, $Mg(OH)_2$, there are only two symmetrically equivalent OH groups and two spectra have been presented (Wirth 1997, van Aken *et al* 1999) which differ from each other significantly. After discussing the reliability of our approach, we then compute the oxygen K-edge spectrum of diaspore, α-AlOOH, and complement the modeling study by the experimental determination of time resolved EEL spectra of diaspore.

2. Computational details

The computational approach employed here has been described in detail by Gao *et al* (2009) and further applications have been given by Milman *et al* (2010). All calculations in the current study were performed using the CASTEP package (Clark *et al* 2005). The PBEsol generalized gradient approximation (Perdew *et al* 2008) and the 'on the fly' pseudopotentials from the CASTEP data base were employed throughout. The kinetic cut-off energy was 610 eV. Distances between k-points for Brillouin zone sampling were <0.03 Å^{-1}. For the EELS calculation, core holes were introduced in subsequent calculations for symmetrically distinct oxygen atoms. As we employed periodic boundary conditions, we used supercells to ensure that the distance between pseudo-atoms with a core hole was at least 6 Å. Convergence calculations showed that larger distances, which are computationally very expensive, only lead to small changes in the spectra. The contributions of symmetrically distinct oxygen atoms were summed up according to the method described by Mizoguchi *et al* (2009). Core hole lifetime effects are included in the spectrum calculation via a Lorentzian broadening with FWHM of 0.19 eV (Fuggle and Inglesfield 1992). The broadening due to the lifetime of an excited state is more complicated. We adopted an empirical linear function that describes broadening width as $0.1E$ where E is the energy above the adsorption threshold (Hebert 2007) in order to describe this effect. The spectrum of a single molecule was obtained by an EELS calculation for a spin-polarized O_2 molecule placed in a $10 \times 10 \times 10$ Å^3 box. The rest of the settings (exchange–correlation functional, energy cut-off, k-point sampling) were the same as for the solid state calculations; instrumental broadening for the single molecule EELS calculation was set at Gaussian FWHM of 0.1 eV.

3. Experimental details

Thin flakes of sample were obtained from a gem-stone quality natural diaspore by treatment in an ultrasonic bath in isopropyl alcohol, then mounted on lacey carbon coated Cu grids. Observations were made on samples with no carbon underneath. The EEL spectra were acquired with a FEI Tecnai F30 transmission electron microscope equipped with a Gatan image filter (GIF). The voltage used was 300 keV and the EELS energy resolution (FWHM) was about 1.0 eV at the minimum dispersion of 0.05 eV and about 1.3–1.4 eV (FWHM) at the usual acquiring dispersion of 0.3 eV/channel. Care was taken to do all necessary alignments in an area adjacent to the area of interest. The time series spectra were done with the beam continuously impinging on the area of interest and acquiring spectra every 30 s. The background was removed from all EEL spectra by polynomial fitting using standard Digital Micrograph procedures.

4. Results and discussion

4.1. Hambergite

The structure of hambergite, $Be_2BO_3(OH)$, an orthorhombic beryllium borate, has been determined by Zachariasen *et al* (1963) and has been refined recently by single crystal neutron diffraction by Gatta *et al* (2012). Experimentally determined structural parameters are given in table 1. There has been no density functional theory based atomistic modeling study of hambergite and hence the results of the full geometry optimization are given in table 1. They are in good agreement with the experimental data (Zachariasen *et al* 1963, Gatta *et al* 2012). Specifically, the computed O–H distance is 0.995 Å, while the neutron diffraction study gave distances between 0.971 and 1.0105 Å, depending on the details of the model used (Gatta *et al* 2012).

The computed EEL spectrum (figure 1) is in good agreement with the experimental spectrum (Garvie 2010) close to the K-edge. The theoretical spectrum was simulated with a uniform broadening of 0.25 eV, and does not account for multiple scattering or any kind of background. This leads to an increasing discrepancy between experiment and theory at higher energies. The individual contributions from symmetrically distinct oxygen atoms bound to the boron differ little from each other. The contribution from the oxygen which is bound to the hydrogen dominates the scattering between the

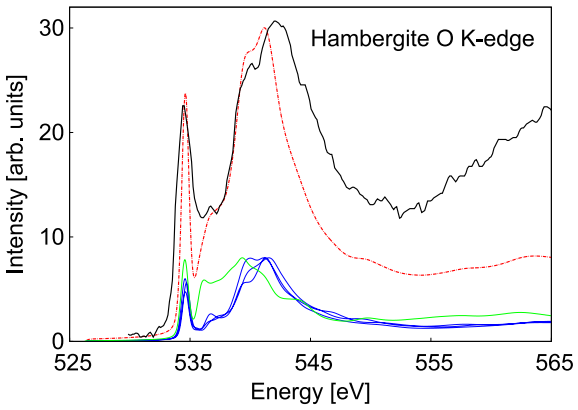

Figure 1. Experimental (black continuous line, Garvie 2010) and theoretical EEL spectra of hambergite. The dashed (red) line representing the total spectrum is the sum of the contributions from the four symmetrically independent oxygen atoms. Three of these oxygen atoms (blue lines) are bound to boron, while one (green line) is part of an OH group. The contribution from the latter dominates the total spectrum between the two main peaks and is distinct from the contributions from the BO_3-group.

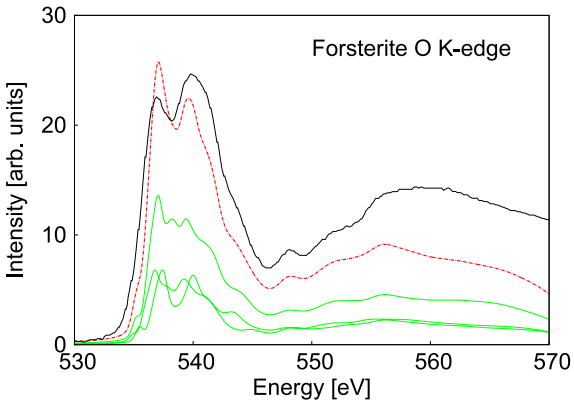

Figure 2. Experimental (continuous (black) line, Garvie 2010) and theoretical EEL spectra of forsterite. The dashed (red) line representing the total spectrum is the sum of the contributions from the three symmetrically independent oxygen atoms (green lines). One set of oxygen atoms occupy Wyckoff position 8d and therefore contributes twice as much as the other two sets of oxygen atoms, which are both located on Wyckoff position 4c.

Table 1. Structural parameters of hambergite from experiment and DFT calculations. The first line for each parameter gives experimental data from Zachariasen *et al* (1963), while the DFT results are shown in the second line. The experimental lattice parameters are $a = 9.755(1)$ Å, $b = 12.201(1)$ Å, and $c = 4.426(1)$ Å, (Zachariasen *et al* 1963), while the corresponding calculated values are 9.7486 Å, 12.0167 Å and 4.4078 Å, respectively.

	x	*y*	*z*
Be	0.0029(4)	0.1882(3)	0.260(1)
	−0.000 865	0.187 165	0.262 265
Be	0.2375(3)	0.0676(3)	0.2775(8)
	0.233 687	0.066 980	0.280 337
B	0.1059(3)	0.1072(2)	0.7719(8)
	0.104 551	0.106 717	0.775 492
O	0.0377(2)	0.1875(1)	0.6199(4)
	0.034 550	0.187 910	0.619 465
O	0.1013(2)	0.1029(1)	0.0815(4)
	0.098 192	0.101 573	0.086 829
O	0.1867(2)	0.0346(1)	0.6181(4)
	0.187 758	0.034 140	0.619 444
O	0.3399(2)	0.1729(1)	0.2956(5)
	0.336 219	0.174 970	0.293 002
H	0.3117(38)	0.2170(33)	0.4554(99)
	0.314 433	0.225 237	0.465 723

two main peaks. It is noteworthy that all oxygen atoms equally contribute to the sharp feature at 535 eV, which is therefore not a pre-peak feature due to the hydrogen.

4.2. Forsterite

Forsterite, Mg_2SiO_4, has been the subject of numerous DFT based modeling studies (Jochym *et al* 2004, Winkler *et al* 1996, Demichelis *et al* 2010, Ashbrook *et al* 2007). It is well established that its physical properties are described well by DFT-GGA based calculations and the results of the geometry optimization of forsterite are in similarly good agreement with experiment as those of hambergite. The computed EEL spectrum is compared to the experimental spectrum (Garvie 2010) in figure 2. The most prominent feature in both the experimental and the theoretical data set is the edge with two maxima, separated by ≈2.6 eV. The intensity ratios of these two main maxima are not well reproduced. However, as the experimental spectrum is neither corrected for background or multiple scattering, and it is not clear whether it represents a proper powder average, these differences are not indicative of a failure of the model. Also, the theoretical spectrum reproduces minor features, such as the shoulder at 543.7 eV, and the local maxima at 548.1 and 551.8 eV.

4.3. Brucite

Brucite, $Mg(OH)_2$, has also been studied extensively by *ab initio* methods (D'Arco *et al* 1993, Winkler *et al* 1995, van Aken *et al* 1999). An EEL spectrum, obtained by Wirth (1997), is shown in figure 3. It has a very prominent feature at energies lower than the oxygen K-edge. The spectrum by Wirth (1997) differs distinctly from the ELNES spectrum published by van Aken *et al* (1999), who obtained spectra on samples with a preferential orientation. Even an adjustment of the onset of the energies of the K-edge doesn't lead to a satisfactory agreement between the two spectra.

The results of our polarized calculations are compared to the data by van Aken *et al* (1999) in figure 4. The intensity distributions are, in part, not well reproduced. However, the theoretical spectra are fully polarized, while this has not been the case for the experimental spectra. In addition, the theoretical model has a perfect alignment of the OH groups parallel to the *c*-axis. This is just a first approximation to the disordered arrangement of the OH groups in the real structure, as neutron diffraction data is best described by models in which the hydrogen atoms are distributed over three sites (Desgranges *et al* 1996, Chakoumakos *et al* 1997). However,

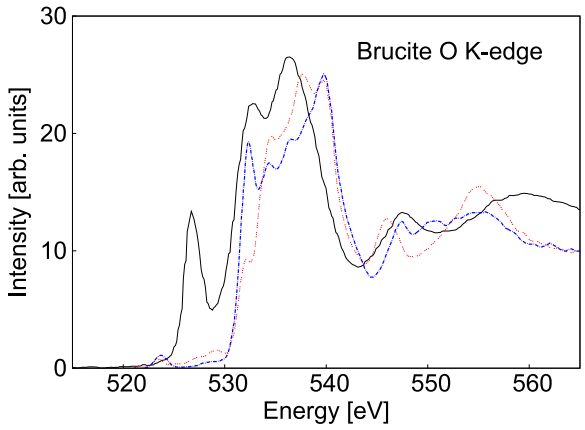

Figure 3. Experimental EEL spectra of brucite. The continuous (black) line with the prominent pre-edge peak is from Wirth (1997). The two spectra from van Aken *et al* (1999), shown by dashed (red and blue) lines, were obtained on samples with a different preferential orientation.

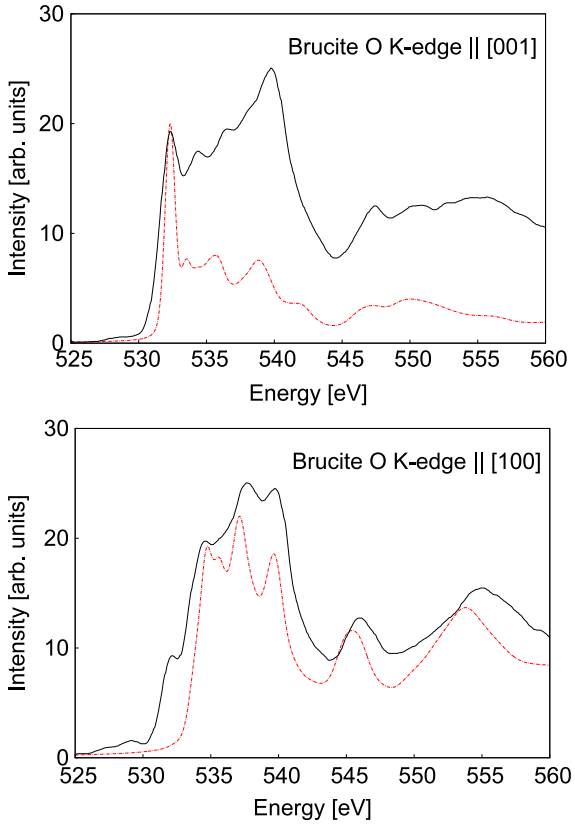

Figure 4. Comparison of theoretical polarized spectra (dashed (red) lines) to the experimental (black, continuous line) spectra obtained on samples with a preferential orientation (van Aken *et al* 1999).

it is obvious that neither in the theoretical spectra, nor in those shown by van Aken *et al* (1999) is there a pre-edge feature due to the O–H bonding, and combining these two results we conclude that the spectrum published by Wirth (1997) is not representative of brucite.

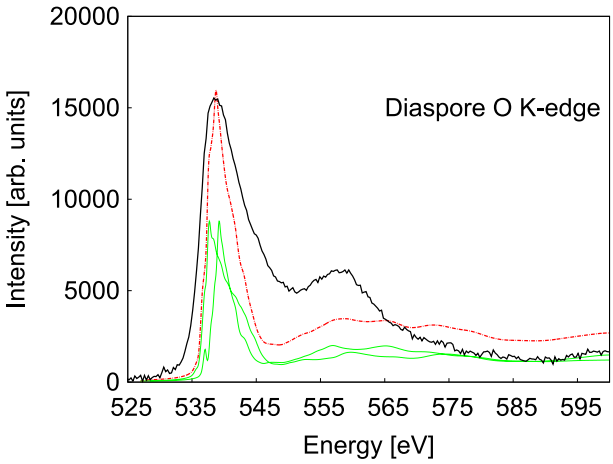

Figure 5. Experimental (continuous black line) and theoretical EEL spectra of diaspore. The dashed (red) line representing the total spectrum is the sum of the contributions from the two symmetrically independent oxygen atoms (green lines), one of which is part of an OH group.

4.4. Diaspore

Diaspore has been studied extensively by experiment (Mao *et al* 1994, Friedrich *et al* 2007a, 2007b, Frost *et al* 1999, Ruan *et al* 2001, Winkler *et al* 2008, San Juan-Farfan *et al* 2011, Delattre *et al* 2012) and theory (Winkler *et al* 1995, 2001, Demichelis *et al* 2007, Delattre *et al* 2012). It is well established that conventional DFT calculations give a very reasonable description of the interatomic interactions, even though anharmonicity is relevant in this system. A comparison of a computed and an experimentally determined EEL spectrum of diaspore, recorded immediately after the electron beam impinged on the sample, is given in figure 5. Both spectra show no pre-edge feature.

However, time resolved EELS (figure 6) showed that for diaspore there is a transient spectral feature at 529.9 eV, which appears after a few tens of seconds of irradiation and then disappears after a further few tens of seconds. This transient feature can be very well modeled with a contribution of molecular O_2 (figure 6).

5. Conclusion

The current study convincingly demonstrates the accuracy with which EEL spectra can be simulated from DFT based calculations. Specifically, the oxygen K-edge spectra of hydrous and anhydrous minerals are well reproduced. A detailed analysis of the individual contributions of the four symmetrically distinct oxygen atoms in hambergite shows that while there are some differences between the contributions to the EEL spectrum of the oxygen atoms which are part of the BO_3-groups and those which are part of OH groups, these cannot be readily discerned in the experimental spectrum. Similarly, the individual contributions to the total EEL spectrum from the two symmetrically distinct oxygen atoms in diaspore, one of which is part of an OH group, could only be observed if the experimental resolution would be an order

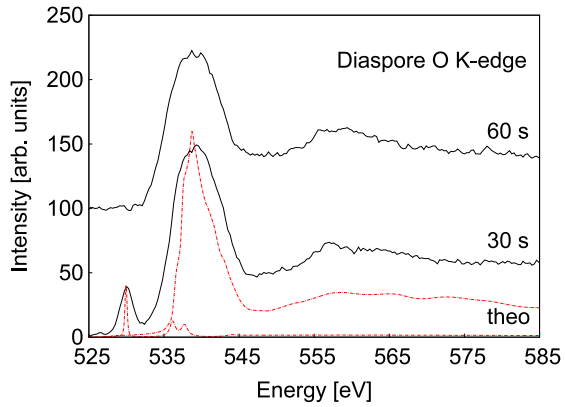

Figure 6. Experimental EEL spectra (continuous black lines) recorded after 30 and 60 s show that, in comparison to a spectrum taken at 0 s (figure 5), a transient feature appears after a few tens of seconds and disappears a few tens of seconds later. This transient feature can be very well modeled by superposing the theoretical EEL spectrum of diaspore on that of molecular O_2 (dashed red lines).

of magnitude better than what is currently achievable. Our experiments on diaspore show the same effect that has been observed by Jiang (2006) on $CaAl_2O_4$, namely a pronounced time-dependent pre-edge feature which can best be explained by assigning it to molecular oxygen, which is liberated by beam damage from the sample. The present study therefore confirms the conclusions drawn by Garvie (2010) on the basis of experimental data, leaving little doubt that the hydrogen content of minerals cannot be determined by EELS through a pre-peak feature in the oxygen K-edge spectrum.

Acknowledgments

BW acknowledges financial support from the Deutsche Forschungsgemeinschaft (DFG), Germany, within project Wi1232. We thank LINAN (IPCyT) for providing access to electron microscopy facilities and N Cayetano for help with TEM work. CJP acknowledges support from the Engineering and Physical Sciences Research Council (EPSRC), UK, under project EP/G007489/2.

References

Ashbrook S E, Le Polles L, Pickard C J, Berry A J, Wimperis S and Farnan I 2007 *Phys. Chem. Chem. Phys.* **9** 1587–98
Chakoumakos B C, Loong C-K and Schultz A J 1997 *J. Phys. Chem.* B **101** 9458–62
Clark S, Segall M, Pickard C, Hasnip P, Probert M, Refson K and Payne M 2005 *Z. Kristallogr.* **220** 567–70
D'Arco P, Causa M, Roetti C and Silvi B 1993 *Phys. Rev.* B **47** 3522–9
Delattre S, Balan E, Lazzeri M, Blanchard M, Guillaumet M, Beyssac O, Haussühl E, Winkler B, Salje E K H and Calas G 2012 *Phys. Chem. Miner.* **39** 93–102
Demichelis R, Civalleri B, Ferrabone M and Dovesi R 2010 *Int. J. Quantum Chem.* **110** 406–15
Demichelis R, Noel Y, Civalleri B, Roetti C, Ferrero M and Dovesi R 2007 *J. Phys. Chem.* B **111** 9337–46
Desgranges L, Calvarin G and Chevrier G 1996 *Acta Crystallogr.* B **52** 82–6
Friedrich A, Haussühl E, Boehler R, Morgenroth W, Juarez-Arellano E A and Winkler B 2007a *Am. Mineral.* **92** 1640–4
Friedrich A, Wilson D J, Haussühl E, Winkler B, Morgenroth W, Refson K and Milman V 2007b *Phys. Chem. Miner.* **34** 145–57
Frost R L, Kloprogge J T, Russel S C and Szetu J 1999 *Appl. Spectrosc.* **53** 829–35
Fuggle J and Inglesfield J (ed) 1992 *Unoccupied Electronic States* (*Topics in Applied Physics* vol 69) (Berlin: Springer)
Gao S P, Pickard C J, Perlov A and Milman V 2009 *J. Phys.: Condens. Matter* **21** 104203
Garvie L A J 2010 *Am. Mineral.* **95** 92–7
Gatta G D, McIntyre G J, Bromiley G, Guastoni A and Nestola F 2012 *Am. Mineral.* **97** 1891–7
Hebert C 2007 *Micron* **38** 12–28
Jiang N 2006 *J. Appl. Phys.* **100** 013703
Jochym P T, Parlinski K and Krzywiec P 2004 *Comput. Mater. Sci.* **29** 414–8
Mao H K, Jinfu S, Jingzhu H and Hemley R J 1994 *Solid State Commun.* **90** 497–500
Milman V, Refson K, Clark S J, Pickard C J, Yates J R, Gao S P, Hasnip P J, Probert M I J, Perlov A and Segall M D 2010 *J. Mol. Struct.: THEOCHEM* **954** 22–35
Mizoguchi T, Tanaka I, Gao S P and Pickard C J 2009 *J. Phys.: Condens. Matter* **21** 104204
Perdew J P, Ruzsinszky A, Csonka G I, Vydrov O A, Scuseria G E, Constantin L A, Zhou X and Burke K 2008 *Phys. Rev. Lett.* **100** 136406
Pickard C J and Payne M C 1997 *Electron Microscopy and Analysis 1997* ed J M Rodenburg (Bristol: Institute of Physics) pp 179–82
Ruan H, Frost R and Kloprogge J 2001 *J. Raman Spectrosc.* **32** 745–50
San Juan-Farfan R E, Bayarjargal L, Winkler B, Haussühl E, Avalos-Borja M, Refson K and Milman V 2011 *Phys. Chem. Miner.* **38** 693–700
van Aken P A, Liebscher B and Styrsa V J 1998 *Phys. Chem. Miner.* **25** 494–8
van Aken P A, Wu Z Y, Langenhorst F and Seifert F 1999 *Phys. Rev.* B **60** 3815–20
Winkler B, Blaha P and Schwarz K 1996 *Am. Mineral.* **81** 545–9
Winkler B, Friedrich A, Wilson D J and Haussühl E 2008 *Phys. Rev. Lett.* **101** 065501
Winkler B, Hytha M, Pickard C, Milman V and Warren M 2001 *Eur. J. Mineral.* **13** 343–9
Winkler B, Milman V, Hennion B, Payne M, Lee M and Lin J 1995 *Phys. Chem. Miner.* **22** 461–7
Wirth R 1997 *Phys. Chem. Miner.* **24** 561–8
Wirth R 1998 *Phys. Chem. Miner.* **25** 499–500
Zachariasen W H, Plettinger H A and Marezio M 1963 *Acta Crystallogr.* **16** 1144–6